DOI: 10.1002/adma.200701715

Non-Lithographic Wrinkle Nanochannels for Protein Preconcentration**

By *Seok Chung, Jeong Hoon Lee, Myoung-Woon Moon, Jongyoon Han,* and *Roger D. Kamm**

Nanofluidic channels offer new opportunities for manipulating small molecules such as DNAs[1] and proteins.[2] However, the fabrication of nanofluidic channels aligned with microfluidic networks currently requires precise lithography and nanofabrication procedures.[2a] To address the need for a simple, low-cost fabrication method for forming close-packed nanofluidic channels, we explored an approach that produces shallow wrinkles on a poly(dimethyl siloxane) (PDMS) substrate. We found that the wrinkle pattern could be created by stretching a sheet of PDMS and then treating the surface with oxygen plasma to generate a stiff skin, largely composed of SiO_x[3] the density of which is approximately half that of silica.[4a] Upon releasing the pre-stress, a sinusoidal wrinkle pattern forms with a well-defined wavelength and an amplitude that exhibits nanometer-scale dimensions. This method of wrinkle formation on a PDMS surface is similar to the method first demonstrated by Efimenko et al.[4a] The apparent advantage is that such wrinkles can be easily formed into wrinkle nanochannels (WNCs) by bonding on other substrate, at a high density without the need for a lithography, etching, or deposition processes, by using only surface treatments with UVO (ultraviolet/ozone), an ion beam, or an oxygen plasma.[4]

Wrinkles were created with varied process values, followed by atomic force microscopy (AFM) measurements to build a design guideline. The process is illustrated in Figure 1. Above the critical stress associated with the onset of wrinkling in the thin stiff layer of approximate thickness t on a PDMS surface, the stiff layer under uniaxial compressive stress would wrinkle in a sinusoidal configuration. The wavelength (L) or width of wrinkle would be determined by the ratio of elastic moduli between the film (E_f) and substrate (E_s) according to[4,5]

$$L/t = \alpha \cdot \sqrt[3]{\overline{E}_f/\overline{E}_s} \quad (1)$$

Here, α is approximately 4.36 and $\overline{E} = E/(1-\nu^2)$.[4a] The elastic moduli are kept constant since the modulus for the stiff layer would be fixed regardless of exposure time.[4] However, with exposure time, the thickness of a stiff surface can be expected to increase with the time. That makes the wavelength (L) to be linearly increasing, based on Equation 1. Note that wrinkle wavelength is decreased by reducing the thickness of the stiff layer or by reducing the ratio of elastic moduli, $\overline{E}_f/\overline{E}_s$, and that the wavelength and therefore the width of WNCs can be controlled by varying surface exposure time.

An analytical prediction for the amplitude (W) or height of the wrinkles under uniaxial strain, is given as[5]

$$W/t = \sqrt{e/e_C - 1} \quad (2)$$

where e and e_c are the applied strain, and the critical strain ($e_C = 1/4(3E_s/E_f)^{2/3}$) for the onset of wrinkling. Consequently, the height of the channel can be controlled by the stretching strain and the thickness of the stiff layer, or treatment time.

Using the theory as a guide, the wavelength and amplitude of wrinkles can be independently controlled by varying strain and exposure time. Briefly, increased exposure times thicken the stiff layer, increasing both the wavelength and the amplitude of the wrinkles. Also, at the same exposure time increasing initial strain produces wrinkles with increasing aspect ratios, (i.e., the ratio of wavelength to amplitude) since strain influences wrinkle amplitude but not wavelength. As predicted, the wavelength (width) and amplitude (height) of the wrinkles measured by AFM varies in proportion to surface exposure time (Fig. 2) under the same strain. The data marked by triangles in Figure 2 show that only amplitude is changed for a fixed exposure time, to maintain a constant wavelength. The aspect ratio increased from 2 to 2.5 at 75% strain to 4.5 to 5 at 50% strain, demonstrating size-controllability of wrinkles trough strain and exposure time.

[*] Prof. R. D. Kamm, S. Chung
Germeshausen Professor of Mechanical and Biological Engineering
Department of Mechanical Engineering and Biological Engineering
Massachusetts Institute of Technology
Cambridge, MA 02139 (USA)
E-mail: rdkamm@mit.edu
J. H. Lee, J. Han
Department of Electrical Engineering and Computer Science
Massachusetts Institute of Technology
Cambridge, MA 02139 (USA)
M.-W. Moon
Division of Engineering and Applied Sciences
Harvard University
Cambridge, MA 02138 (USA)
M.-W. Moon
Future Fusion Technology Laboratory
Korea Institute of Science and Technology
136-791 (Korea)

[**] S.C. was supported by an IT Scholarship Program supervised by the IITA (Institute for Information Technology Advancement) & MIC (Ministry of Information and Communication), Korea. J.H.L. received support by NIH grants R01-EB005743, P30-ES002109-28 (MIT-CEHS), and a Korea Research Foundation grant (KRF-2005-000-10051-0).

ADVANCED MATERIALS

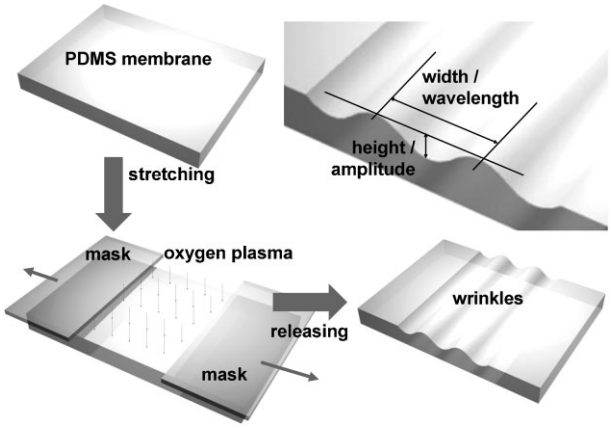

Figure 1. Wrinkle generation on a bare PDMS plate. Under uniform stretching, the PDMS layer is covered by a mask, exposed to oxygen plasma, and then released slowly. The exposed region on the PDMS generates wrinkles with controllable dimension. The terms of wavelength and amplitude are defined by width and height of the wrinkles, measured by AFM.

The wrinkles generated on the bare PDMS substrate or those with microfluidic patterns were covered by another substrate to form integrated systems with a combination of wrinkle nanochannels (WNCs) and microfluidic channels. With masking, wrinkles could be confined to a desired 2 mm wide region between the microfluidic channels. Details for two different fabrication methods are illustrated in Figure 3a and b and in the Experimental section. A complementary approach was published by Huh et al.,[6] who used cracks that form in the oxide layer on PDMS to make tuneable tunnels to selectively

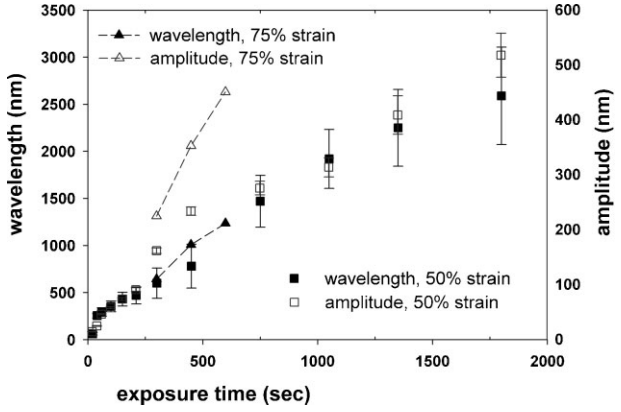

Figure 2. Graph of wavelength (width) and amplitude (height) of the wrinkles as a function of exposure time to oxygen plasma. Dimensions measured by AFM. The value of the amplitude in all strains can be acquired from the right axis, and that of wavelength from the left axis. Under 50% strains, wavelength and amplitude data indicated by squares show a stable increase, keeping an aspect ratio of 4.5–5.0 (ratio with wavelength over amplitude). Under 75% strain, only amplitude data indicated by triangles are increased, remaining wavelength not changed and also keeping an aspect ratio of 2–2.5.

manipulate nanometer-sized DNA molecules and quantum dots. In their study, cracks were formed by stretching after oxidation of PDMS with dimensions approximately 700 nm wide and 80 nm high, and the shape was copied onto a PDMS surface through a series of replication steps. The PDMS layer with crack patterns was then placed against another flat substrate and pressure was applied to modulate the size of reversibly bonded nanofluidic channels. While a method was proposed for generating the channels, they did not suggest, however, how to control the size, spacing, and position of the cracks. They could reduce the channel size by applying pressure on the assembled device, but it is not clear if this is reversible. Thus, wrinkles can be a simpler and more controllable alternative. Compared to cracks, the size and spacing of the wrinkles can be precisely controlled from several tens of nanometers to micrometers. Wrinkles can also be confined to specific regions on the PDMS surface for integration with other microfluidic circuits (Fig. 4a).

WNCs created by cover-plate bonding have triangular cross-sections (Fig. 4b) and a reduced width/height in comparison with the original wavelength/amplitude of wrinkles owing to the bonding. Before bonding the dimension of wrinkles made with an exposure time of 4800 seconds was 8.6 μm wide and 1 μm high with an aspect ratio of 8.6. After bonding, the larger closed WNCs maintained their initial aspect ratio. However, smaller WNCs, for example those forming about 3990 nm wide and 202 nm high with an aspect ratio of about 20 (2400 s of exposure time), had a reduced size after bonding (Fig. 4c). Smaller-sized WNCs made from wrinkles (950 nm wide and 233 nm high, 450 s of exposure time) also had reduced dimensions after bonding, to about 955 nm wide and 52 nm high with an aspect ratio of about 20 (Fig. 4d). The observed tendency for the aspect ratio to increase with smaller wrinkles is related to the thinner stiff layer made by shorter plasma exposure times,[6] thereby leading to increased deformation (flattening) of the wave peaks. In addition, van der Waals forces tended to increase the adhesive attraction between wrinkles and substrate.[7] The height of the smallest WNCs we could reliably produce and measure by SEM was about 50 nm.

Nanochannels fabricated in this way could have numerous applications.[1,2] Here, to demonstrate their functionality, we employed them to concentrate a protein solution by using electrokinetic trapping in combination with nonlinear electro-osmotic flow at the anodic side of the system.[2] It is widely recognized that simple and efficient sample concentration tools are essential for the application of proteomics in a biological system, since major challenges for biosensors and assays lie in the enhancement of detection sensitivity for highly diluted analytes.[2b] Recently, preconcentration schemes utilizing permselectivity of a nanochannel was demonstrated by several groups. Pu et al. experimentally demonstrated that both cationic and anionic dyes can be enriched at the cathodic end of a nanochannel and excluded at the anodic side, when a permselective nanochannel current is induced.[8a] More recently, we employed electrokinetic trapping through utilizing

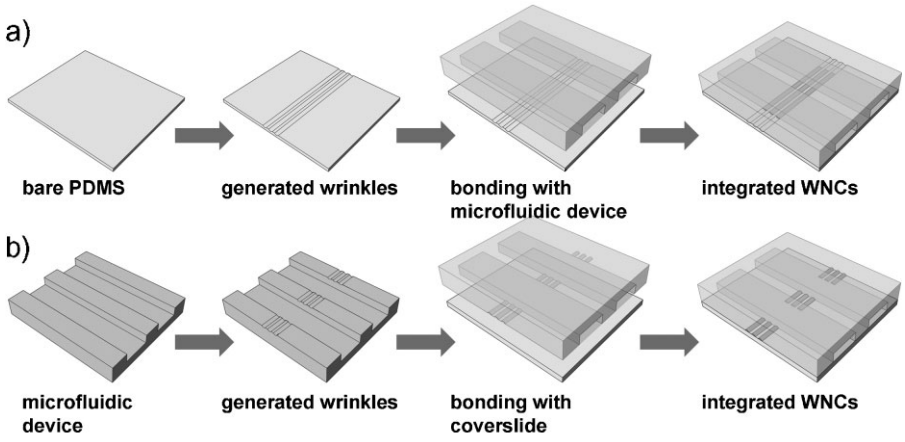

Figure 3. Two schemes to generate wrinkles and integrate them with microfluidic channels. a) Wrinkles can form on the plain PDMS substrate which is subsequently bonded to a second PDMS layer with microfluidic channels or b) can be created directly on the desired area between microfluidic channels and bonded to a flat substrate. Wrinkles can be generated over an entire surface, or locally in a specific region.

depletion behavior at the anode side of the nanochannel,[2a] demonstrating protein preconcentration amplification by a factor of 1 million. To demonstrate the utility of WNC systems for protein preconcentration, we used a system shown schematically in Fig. 5a. The WNCs are formed between two microchannels (50 μm wide and 20 μm deep) and all channels are filled with β-phycoerythrin (β-PE) protein (4 nM) in phosphate buffer (10 mM, pH 7.0). In order to concentrate

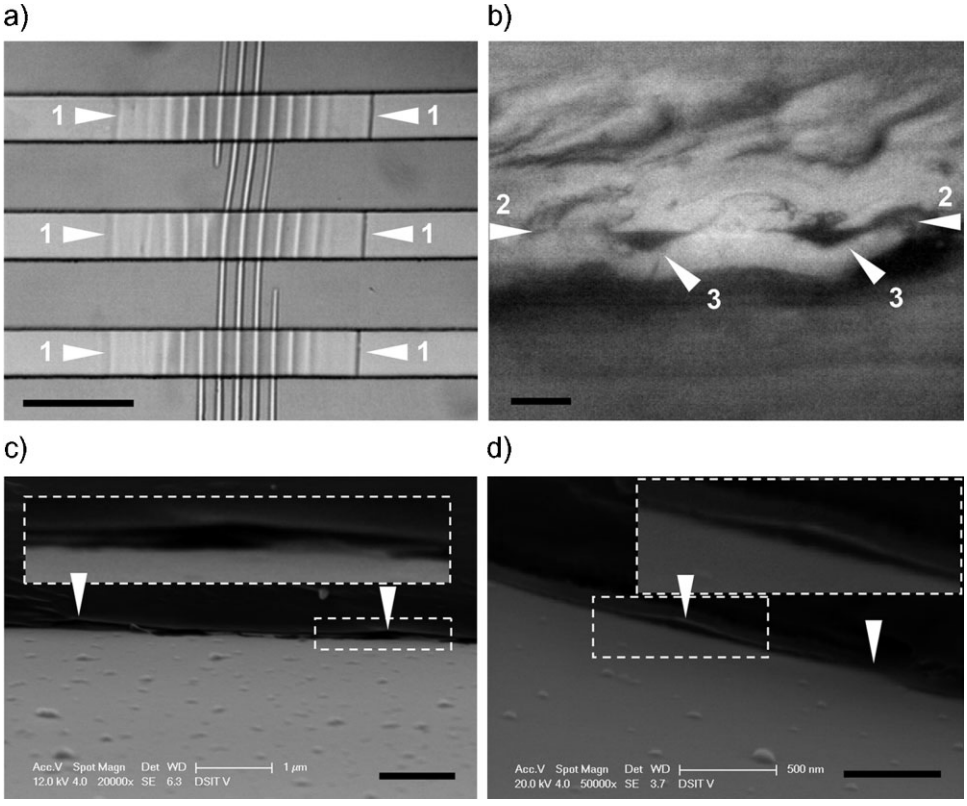

Figure 4. a) Microfluidic channels matched with WNCs prepared by an exposure time of 4800 seconds (8600 nm wide and 989 nm high). White triangles #1 mark the interface defined by transparency film during plasma exposure. The wrinkles were generated only in the region between the interfaces and bonded to the top PDMS layer with microfluidic channels. Scale bar = 50 μm. b) Magnified cross-sectional view of WNCs, showing the triangular cross-section. White triangles #2 indicate the interface between top and bottom PDMS layer and #3 indicate the WNCs. Scale bar = 3 μm. Picture taken by optical microscopy. c) SEM picture of WNCs made with wrinkles (2400 seconds of exposure time). Scale bar = 1 μm. d) SEM picture of WNCs made with winkles (450 s of exposure time). The height of the WNCs was measured to be an average of 52 nm. Scale bar = 500 nm. The substrate of (c) and (d) is a glass coverslide. The white triangles in (c) and (d) indicate peaks of WNCs.

ADVANCED MATERIALS

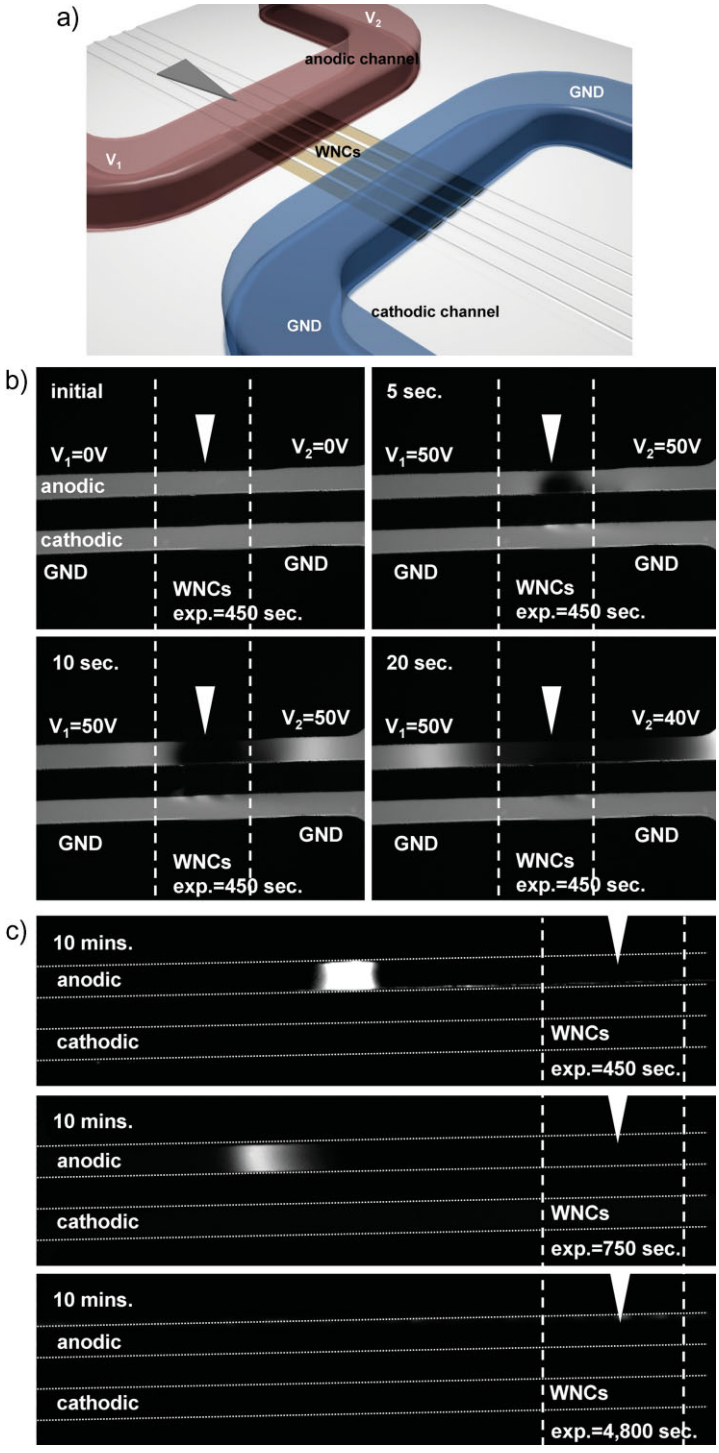

Figure 5. a) Schematic showing the device used for protein preconcentration, consisting of the WNCs and microfluidic channels. Triangles indicate the center position of the anodic channel; the same position indicated by white triangles in (b) and (c). b) Time-dependent formation of protein plug formed near the WNCs. Numbers in top-left side represent the concentration time. GND (ground), 0 V, 40 V, and 50 V indicate the voltage applied at the inlet/outlet connected to the channels. The WNCs were formed in a 2 mm wide region between the microfluidic channels, indicated by dashed lines. Numbers under WNCs indicate the exposure time for generating wrinkles used for concentration. c) Fluorescent pictures of protein preconcentration plugs taken in 10 min of concentration time. The WNCs formed region and center position of the anodic channel are also indicated by dashed lines and white triangles. Another thin dashed line shows the position of anodic and cathodic channels. Numbers in left top side mean the concentration time and those under WNCs mean exposure time for generating wrinkles used in concentration. Winkle dimensions before bonding generated by each treatment time are, 450 s; 900 nm wide and 233 nm high, 750 s; 1,470 nm wide and 275 nm high, 4800 s; 8600 nm wide and 989 nm high. Height of WNCs formed of wrinkles with exposure time of 450 seconds is an average of 52 nm (Fig. 4d). The smallest wrinkles (top) generate the brightest signal, which means the highest preconcentration ratio, while the biggest wrinkles (bottom) generate nothing.

the protein, we initially applied 50 V onto two anodic side reservoirs, while the others were grounded (Fig. 5b). Then, we induced a tangential force onto microfluidic channel in the anodic side by changing voltage of one reservoir (from 50 V to 40 V), resulting in fast accumulation of biomolecules in front of the induced space-charge layer (Fig. 5c). As can see in Figure 5b, a depletion zone is generated near WNCs. When an electric field is applied across the nanochannel, the nanochannel shows an ion-permselectivity by an electrical double layer overlapping and consequently pumps only positive ions in case of zeta-potential of nanochannel is negative. We used 10 mM buffer solution and were able to acquire the depletion formation near the WNCs in an anodic side. Also we observed expansion of the depletion zone with time. The Debye length (λ_D) is about 3 nm in 10 mM phosphate buffer solution.[8b] The formation of the depletion zone occurs only in the case that the size of the electrical double layer (ca. 3 nm in case of 10 mM buffer solution) is comparable to the channel size. Evidently, WNCs could be used for ion permselective nanochannels of tens of nanometer in size, since the depletion formation (exclusion of ions) is correlated to the nanochannel size.

Preconcentration of β-phycoerythrin protein occurs in a time-dependent manner that is also affected by exposure time, as shown for three different WNC conditions (450, 750, and 4800 s) in Figure 5c, clearly demonstrating that WNC size affects permselectivity. Using the small WNCs made with 450 s exposure time, we acquire the highest preconcentration factor among these three WNCs with time. In contrast, WNCs generated by 4800 s exposure time failed to produce any significant depletion and preconcentration (Figs. 5c and 6). In two other cases, generated from 450 s and 750 s exposure time, preconcentration of protein varied almost linearly in time. The maximum preconcentration factor from the device with wrinkles made by 450 s exposure time is about 10^2. The WNCs made from wrinkles of 470 nm wide and 90 nm high (210 s of plasma exposure time) could also show signs of electrokinetic flow, but could not be reliably made and characterized by SEM owing to their small size. Below this size WNCs collapsed completely, showing no signs of electrokinetic flow.

The major advantage of WNC devices lies in the simple prototyping of nanochannel systems. Moreover, it also demonstrates that WNCs can be integrated with microfluidic channels forming a functional and uniform nanochannel array. Without any lithographic process, we can create nanochannels integrated with microfluidic circuits. Compared to other direct or imprint lithography processes,[9] WNCs can easily form uniform arrays of high density with controllable dimensions in only a specific region. The added flexibility for making a range of nanochannel dimensions on one substrate can also provide opportunities for new applications in nanofluidics. Wrinkles, once considered an undesired artifact in semiconductor production, can now be precisely controlled and used to create densely arrayed nanofluidic channels in a simple, one-step, cost-effective process, providing a more precise manner to handle nanometer-sized molecules.

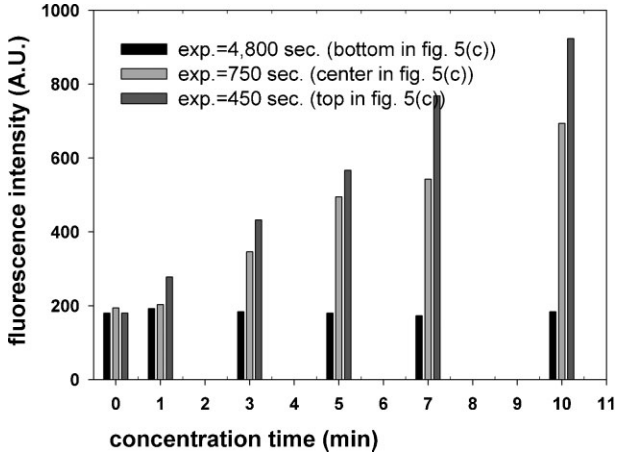

Figure 6. Protein preconcentration result shown as a function of time. The WNCs made from less-exposed (smaller) wrinkles can generate faster increases of fluorescence intensity.

Experimental

Generating Wrinkles and WNCs: We applied strain to a bare PDMS sheet (0.5 mm thick) by a home-made stretching apparatus, and then subjected the sheet to plasma treatment (PDC-32G Cleaner/Sterilizer, Harrick Plasma, NY, USA). The plasma was ignited by normal air showing a bright pink color. Before applying plasma treatment, a transparency film (3M) was cut and attached to the stretched PDMS surface to mask regions where wrinkles were not desired from plasma exposure. After plasma treatment strain was released, resulting in wrinkles on exposed PDMS surface (Fig. 1). To create the homogeneous WNCs of PDMS (Fig. 3a), the wrinkled PDMS layer was bonded onto the other PDMS layer with microfluidic channels. The layers were plasma-treated again for 30 s by the same plasma cleaner and bonded together to form nanochannels aligned with microfluidic channels. To create inhomogeneous nanofluidic channels (Fig. 3b), with three sides made from PDMS and one side made from glass, we applied strain directly on the PDMS layer with microfluidic channels, covered undesired region by the trimmed transparency film and exposed it by the plasma. The wrinkled PDMS layer with microfluidic channels was then bonded to glass coverslide. Wrinkle dimension was measured by atomic force microscopy (AFM, Veeco Instrument Inc., NY, USA) and WNCs dimension was measured by scanning electron microscopy (SEM, FEI/Philips).

Protein Preconcentration: A PDMS layer with two microfluidic channels, one anodic and the other cathodic, was patterned by a general soft lithographic process on SU-8 2050 negative photoresist (Microchem, MA, USA) patterned wafers. Height of the microfluidic channels was 20 micrometers. The channels were then connected by WNCs by the method described above (Fig. 3b). β-Phycoerythrin (molecular weight 240 kDa and p$I = 4.3$) was mixed with phosphate buffer (10^{-2} M, pH 7.0), to make β-phycoerythrin solution (40 nM). The solution was filled into the channels by syringe and platinum electrodes were connected to both inlets and outlets. Applied voltage was controlled using a custom power distributor and power supply from 0 V to 50 V. The concentration plug was analyzed by using fluorescence microscopy.

Received: July 13, 2007
Revised: February 8, 2008
Published online: June 19, 2008

[1] a) J. Han, H. G. Craighead, *Science* **2000**, *288*, 1026. b) M. Foquet, J. Korlach, W. Zipfel, W. Webb, H. G. Craighead, *Anal. Chem.* **2002**, *74*, 1415. c) J. P. Fu, R. B. Schoch, A. L. Stevens, S. R. Tannenbaum, J. Han, *Nat. Nanotechnol.* **2007**, *2*, 121. d) J. Fu, P. Mao, J. Han, *Appl. Phys. Lett.* **2005**, *87*, 263902. e) L. J. Guo, X. Cheng, C. F. Chou, *Nano Lett.* **2004**, *4*(1), 69.

[2] a) Y. C. Wang, A. L. Stevens, J. Han, *Anal. Chem.* **2005**, *77*, 4293. b) J. H. Lee, S. Chung, S. J. Kim, J. Han, *Anal. Chem.* **2007**, *17*, 6868.

[3] M. Ouyang, R. J. Muisener, A. Boulares, J. T. Koberstein, *J. Membr. Sci.* **2000**, *177*, 177.

[4] a) K. Efimenko, M. Rackaitis, E. Manias, A. Vaziri, L. Mahadevan, J. Genzer, *Nat. Mater.* **2005**, *4*, 293. b) M.-W. Moon, S. H. Lee, J.-Y. Sun, K. H. Oh, A. Vaziri, J. W. Hutchinson, *Proc. Natl. Acad. Sci. USA* **2007**, *104*, 1130.

[5] a) N. Bowden, S. Brittain, A. G. Evans, J. W. Hutchinson, G. M. Whitesides, *Nature* **1998**, *393*, 146. b) E. Cerda, L. Mahadevan, *Phys. Rev. Lett.* **2003**, *90*, 074302.

[6] D. Huh, K. L. Mills, X. Zhu, M. A. Burns, M. D. Thouless, S. Takayama, *Nat. Mater.* **2007**, *6*, 424.

[7] H. Hillborg, J. F. Ankner, U. W. Gedde, G. D. Smith, H. K. Yasuda, K. Wikstrom, *Polymer* **2000**, *41*, 6851.

[8] a) Q. Pu, J. Yun, H. Temkin, S. Liu, *Nano Lett.* **2004**, *4*, 1099. b) A. Bard, L. R. Faulkner, *Electrochemical Methods: Fundamentals and Applications*, 2nd ed., Wiley, New York, NY **2001**.

[9] C. M. Sotomayor Torres, *Alternative Lithography*, (Eds: C. M. Sotomayor Torres), Kluwer Academic/Plenum Publishers, New York, NY **2003**, Ch. 1.